

## DYNAMIC PILE-SOIL-PILE INTERACTION. PART I: ANALYSIS OF AXIAL VIBRATION

GEORGE GAZETAS AND NICOS MAKRIS

*National Technical University, Athens, Greece; and Dept Civil Engineering, 212 Ketter Hall, State University of New York, Buffalo, New York 14260, U.S.A.*

### SUMMARY

Simple methods of analysis are developed for computing the dynamic steady-state axial response of floating pile groups embedded in *homogeneous and non-homogeneous* soil deposits. Physically-motivated approximations are introduced to account for the interaction between two individual piles. It is found that such an interaction arises chiefly from the 'interference' of wave fields originating along each pile shaft and spreading outward. For homogeneous deposits the wave fronts originating at an individual pile are cylindrical and the interaction is essentially independent of pile flexibility and slenderness. For non-homogeneous deposits the wave fronts are non-cylindrical and ray-theory approximations are invoked to derive pile flexibility-dependent interaction functions.

Results are presented for the dynamic stiffness and damping of several pile groups, as well as for distribution of the applied load among individual piles. For deposits with modulus proportional to depth, the agreement with the few rigorous solutions available is encouraging. A comprehensive parameter study focuses on the effects of soil inhomogeneity and pile-group configuration. It is demonstrated that the 'dynamic group efficiency' may far exceed unity at certain frequencies. Increasing soil inhomogeneity tends to reduce the respective resonant peaks and lead to smoother interaction functions, in qualitative agreement with field evidence.

### INTRODUCTION

The harmonic response of pile groups is substantially affected by the dynamic interaction between the individual piles. Following the early numerical studies by Wolf and Von Arx<sup>1</sup> and Nogami,<sup>2</sup> several researchers have developed a variety of computational (rigorous and simplified) methods for assessing the pile-soil-pile interaction and computing the dynamic impedances of pile groups.<sup>3-16</sup> The corresponding static problem was treated in References 17-19. The methods developed in these studies differ from one another in the simplifications introduced when modelling this complicated boundary value problem. They are all of an essentially numerical nature as they invariably involve discretizing each pile and the supported soil; hence, application of even the most simplified of them may entail some substantial computational effort, while in some cases these methods rely on proprietary computer codes.

By contrast the analytical solution outlined herein was conceived while trying to explain in the classroom, in very simple physical terms, the causes of the numerically-observed 'resonant' peaks in the dynamic impedances of pile groups. But, the developed elementary explanation of pile-to-pile interaction in *homogeneous* soils leads to results in remarkable accord with rigorous solutions for a number of pile-group configurations, and a fairly wide range of material parameters, pile separation distances and frequencies of vibration. Naturally, the developed simple method has its limitations; a comparative study documenting/calibrating its performance for pile groups in a homogeneous halfspace and a homogeneous stratum has been presented by Dobry and Gazetas.<sup>20</sup> This paper (i) presents analytical *evidence* in support of the crucial assumptions introduced for a *homogeneous* halfspace by Dobry and Gazetas; (ii) extends the method to pile groups in *non-homogeneous* deposits, and compares its predictions against the limited published rigorous results for a halfspace whose modulus increases linearly with depth; and (iii) offers a parametric study to illustrate the significance of soil inhomogeneity and pile flexibility on pile-to-pile interaction.

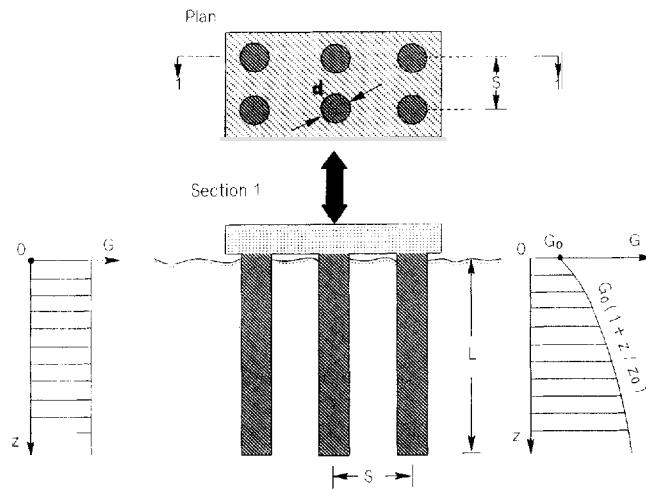


Figure 1. Problem geometry definition and the studied shear-modulus profiles. In all cases, soil Poisson's ratio,  $\nu$ , mass density,  $\rho$ , and hysteretic damping ratio,  $\beta$ , are assumed independent of depth. The piles are treated as elastic flexural beams

Figure 1 illustrates the problem addressed in this paper: studying the forced vertical harmonic oscillation of any group of vertical floating piles embedded in homogeneous or non-homogeneous soil. Note that as a result of pile-to-pile interaction, the distribution of the load to the individual piles will, in general, be non-uniform, as a function of the frequency of oscillation.

### INTERACTION BETWEEN PILES IN A HOMOGENEOUS DEPOSIT: TWO CRUCIAL ASSUMPTIONS

To determine the interaction between pile 'a' and pile 'b', lying at an axis-to-axis distance  $S$  apart, we seek the harmonic head displacement  $W_{12} \exp(i\omega t)$  of pile 'b' due (exclusively) to waves emanating from the circumference of pile 'a'; the latter is forced into a harmonic vertical head displacement  $W_{11} \exp(i\omega t)$ , the complex amplitude of which can be derived from the impedance  $\mathcal{N}^{(1)}$  of the single pile.

To this end, several physically-motivated simplifying assumptions are introduced. Justification of the most crucial of them is provided herein. Specifically:

(a) It is assumed that only cylindrical SV waves are emitted from the oscillating pile 'a', and propagate radially, in the horizontal direction ( $r$ ) only. This hypothesis is reminiscent of the shearing of concentric cylinders around statically loaded piled and pile groups assumed by Randolph and Wroth,<sup>21,22</sup> and is also somewhat similar to the 'Winkler' assumption introduced by Novak<sup>23</sup> and already extensively used with success in dynamic analyses of pile groups.<sup>2,7</sup>

(b) It is further assumed that these cylindrical waves emanate *simultaneously* from all points along the pile length; hence, for a homogeneous deposit, they spread out in-phase and form a *cylindrical wavefront*, concentric with the generating pile. Of course, unless the pile is rigid, the amplitude of oscillation along the wavefront will be a (usually decreasing) function of depth, as illustrated in Figure 2(a). A direct consequence of these assumptions: the shape of the variation of wave amplitude with depth along the cylindrical front remains unchanged as the wavefront expands in a homogeneous medium.

The most crucial assumption, namely, that the waves are sent off *simultaneously* from the circumference of the 'source' pile, is discussed herein.

To begin with, for relatively short (say,  $L/d < 10$ ) and stiff ( $E_p/E_s > 8000$ ) piles the validity of this simplifying assumption is self-evident, since such piles respond essentially as rigid bodies to axial loading—static or dynamic. To show that for a fairly broad range of pile lengths and flexural rigidities this assumption is still an adequate engineering approximation, a rigorous finite-element study is performed. For a pile with

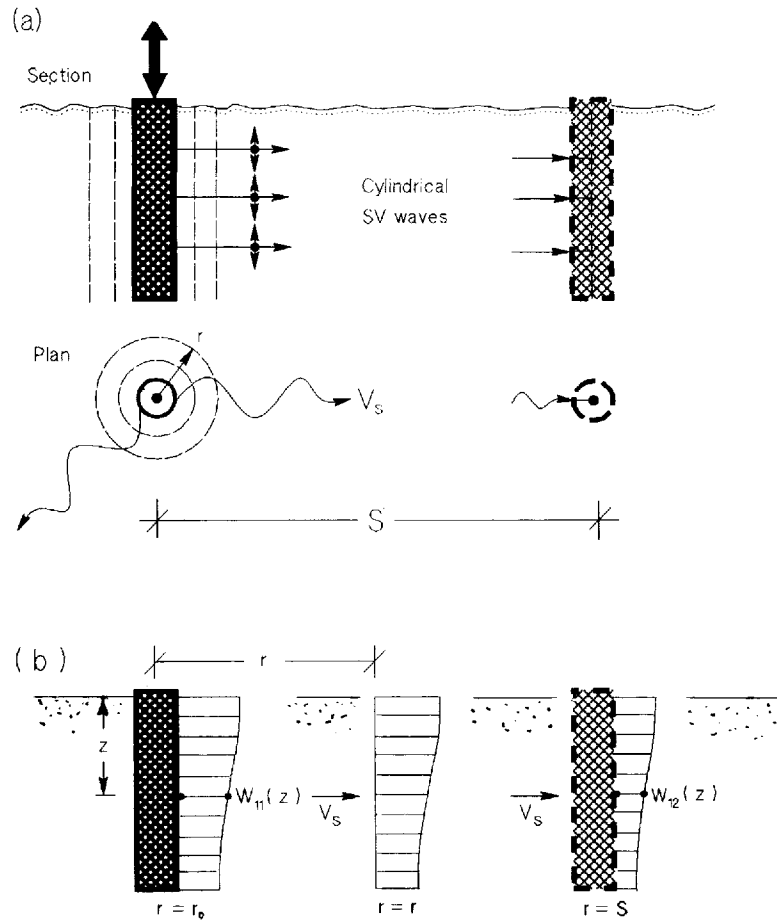


Figure 2. Schematic illustration of the 'cylindrical wavefront' concept that forms the basis of the developed simplified method for pile-to-pile interaction in a homogeneous medium: (a) spreading of SV waves from the oscillating pile; (b) the distribution of displacement amplitudes with depth retains a constant shape as the waves propagate radially and eventually reach the neighbouring pile

slenderness ratio  $L/d = 20$  and  $E_p/E_s = 1000$  and  $5000$ , Figure 3 plots the distribution along the length of the pile of the real and imaginary parts of the vertical pile displacement,  $w = w(z)$ , for two values (0.20 and 0.50) of the frequency factor  $a_0 = \omega d/V_s$ . Evidently, the imaginary component of  $w$  and the resulting phase angle remain nearly constant with depth; hence, the *phase-angle differences* between various points along the pile (also plotted in the figure) are indeed very small, confirming the proposed assumption. Of course, with much longer and softer piles, and at high frequency factors, one should expect these phase differences to grow larger and the assumption of 'synchronous' wave emission, on which the developed method is based, to be correspondingly less accurate.

To get a further insight into the behaviour of relatively long and flexible piles, consider a very long pile supported by continuously distributed 'springs' and 'dashpots' that simulate the dynamic stiffness ( $k_s$ ) and radiation damping ( $c_s$ ) of the surrounding soil. From Angelides and Roesset,<sup>24</sup> Gazetas and Dobry<sup>25</sup> and Kanakari<sup>26</sup>

$$k_s \approx 0.6 E_s (1 + \frac{1}{2} \sqrt{a_0}) \tag{1}$$

$$c_s \approx a_0^{-1/4} \pi d \rho V_s \tag{2}$$

The latter value applies in reality only for frequencies beyond the cutoff frequency  $\omega_c$ , that is, the natural

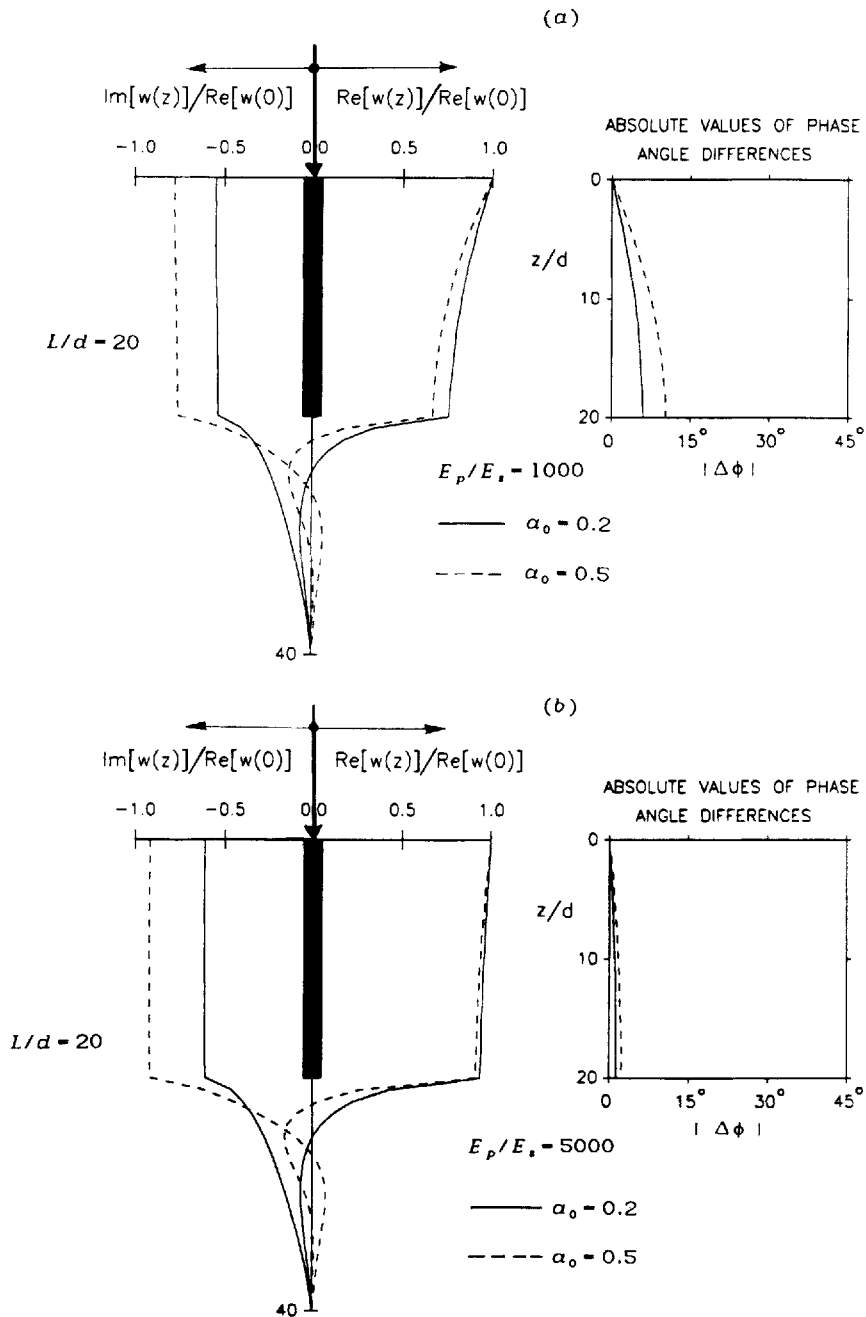


Figure 3. Distribution with depth of normalized vertical pile displacements (Imaginary part and Real part) and pile-displacement phase angle differences for an  $L/d = 20$  pile in a deep homogeneous soil with: (a)  $E_p/E_s = 1000$ ; and (b)  $E_p/E_s = 5000$ . Displacements of soil under the pile are also plotted. Results were obtained with a dynamic finite element formulation for the two shown values of the frequency factor

frequency in vertical vibration of the soil deposit, while for  $\omega < \omega_c$  radiation damping is vanishingly small, and is a function of the (herein neglected) material soil damping.

The governing equation of the steady-state vibration  $w(z)\exp(i\omega t)$

$$E_p A_p \frac{d^2 w(z)}{dz^2} - (k_s + i\omega c_s - m_p \omega^2) w(z) = 0 \tag{3}$$

where  $m_p = \rho_p A_p$  is the mass of pile per unit length. For the only interesting case of  $\omega^2 < k_s/m_p$  (which is valid as long as  $a_0 \leq 1$ ), the solution to equation (3) that respects the radiation conditions takes the form

$$w(z) = W_0 \exp\left(-R \cos \frac{\theta}{2} z\right) \exp\left(-iR \sin \frac{\theta}{2} z\right) \quad (4)$$

where  $W_0 = w(0)$  is the amplitude of pile-head displacement, and

$$\theta = \arctan\left(\frac{\omega c_s}{k_s - m\omega^2}\right), \quad 0 < \theta < \frac{\pi}{2} \quad (5a)$$

$$R^4 = \frac{(k_s - m\omega^2)^2 + (\omega c_s)^2}{(E_p A_p)^2} \quad (5b)$$

Equation (4) represents a travelling wave of exponentially decreasing amplitude with depth. The 'travelling' phase velocity  $C_\alpha$  is

$$C_\alpha = \frac{\omega}{R \sin \frac{\theta}{2}} \quad (6)$$

Below the stratum cutoff frequency, when  $c_s \approx 0$ , this case reduces to the one discussed by Wolf,<sup>27,28</sup> for which

$$C_\alpha \rightarrow \infty \quad (7)$$

Thus, even in a very long pile, waves originating at the top propagate down the pile shaft at a *nearly infinite phase velocity*. Hence all points along the pile perimeter would move essentially in phase.

In general, however,  $C_\alpha$  from equation (6) is finite. For a pile with  $L/d = 20$ ,  $E_p/E_s = 1000$  and  $\rho_p = 1.35\rho$ , equation (6) yields  $C_\alpha/V_s$  values that range between 91 and 123 for  $a_0$  varying in the range of 0.2 to 1. Thus, on the average  $C_\alpha/V_s \approx 100$  and the error committed by assuming 'synchronous' emission would be on the order of 5 per cent, for  $S/d = 4$ . This is an acceptable error for this simple method. A complete study of this problem is presented in Reference 29.

With the foregoing assumptions, the variation of wave amplitude with depth along the cylindrical wavefront arriving at the 'receiving' pile 'b' is analogous to the amplitude variation of the 'source' pile 'a'. As a result, the following approximate expressions are derived for the pile-to-pile dynamic interaction factor,  $\alpha_v$ :

$$\begin{aligned} \alpha_v &\equiv \frac{W_{12}}{W_{11}} \approx \frac{H_0^{(2)}(\omega S/V_s^*)}{H_0^{(2)}(\omega r_0/V_s^*)} \\ &\approx \left(\frac{r_0}{S}\right)^{1/2} \exp\left(-\beta\omega \frac{S}{V_s}\right) \exp\left(-i\omega \frac{S}{V_s}\right) \end{aligned} \quad (8)$$

where  $V_s^* = V_s(1 + 2i\beta)^{1/2}$  and  $H_0^{(2)}$  denotes the zero-order second-kind Hankel function. The last expression, deriving from the asymptotic expansion of the Hankel functions, is a little easier to use and reveals that the amplitude of the interaction factor decays in proportion to the square root of  $S/r_0$  times a hysteretic-damping-dependent exponential decay factor. Moreover, the two expressions lead to only marginally different results. Hence, in view of the desired simplicity of the method, the latter expression has been adopted herein, as in Reference 20.

Equation (8) is sufficient for computing the vertical response of any group of piles, once the response of a single (solitary) pile is known. To this end, the superposition procedure developed for statically loaded groups<sup>17,18</sup> is assumed applicable for dynamic loading as well—an assumption adequately verified by Kaynia<sup>4</sup> and Sanchez-Salineró.<sup>11</sup>

To substantiate the developed method and, thus, provide further (indirect) support for the previously discussed crucial assumption, we present Figure 4. For a 2 by 2 and a 3 by 3 pile group with  $L/d = 15$  and  $E_p/E_s = 1000$  the complex vertical impedances  $\mathcal{X}^{(n)}$ , where  $n$  = number of piles in the group, are cast in the general form

$$\mathcal{X}^{(n)} = \bar{K}^{(n)} + i a_0 C^{(n)} \quad (9)$$

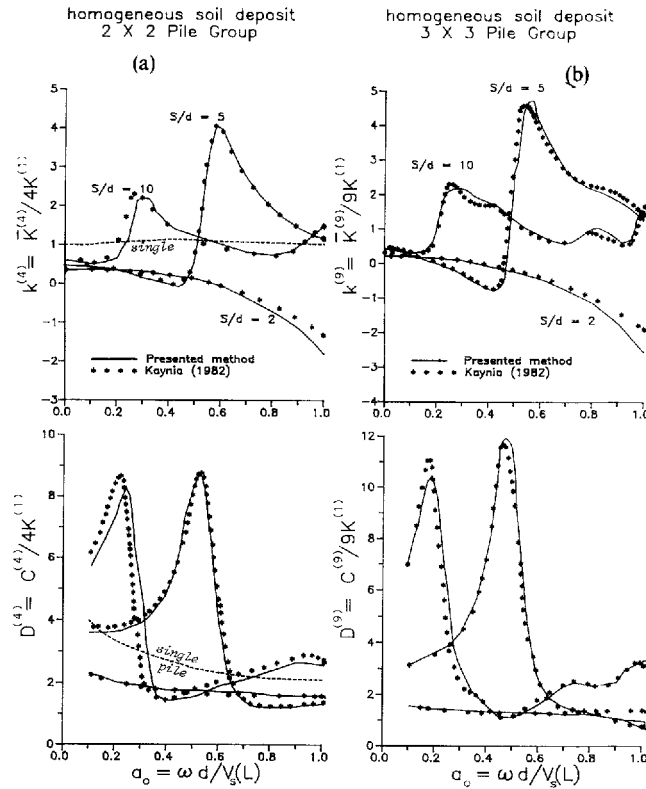


Figure 4. Dynamic stiffness and damping group factors as functions of frequency: comparison of present method with rigorous solution of Kaynia<sup>4</sup> for two square groups of rigidly-capped piles in a homogeneous halfspace.  $E_p/E_s = 1000$ ,  $L/d = 15$ ,  $\beta_s = 5$  per cent. Adapted from Reference 20. The dashed lines are for the solitary single pile

where  $\bar{K}^{(n)}$  is the dynamic group stiffness, and  $C^{(n)}$  is the group damping coefficient which encompasses both geometric and hysteretic ( $\beta = 0.05$ ) dissipation of energy. (In Figure 4,  $n = 4$  and 9.) Define the 'dynamic stiffness group factor',  $k^{(n)}$ , and the 'damping group factor',  $D^{(n)}$ , as the ratios of the dynamic stiffness and damping coefficients, respectively, to the sum of the static stiffnesses of the individual single piles:

$$k^{(n)} = \frac{\bar{K}^{(n)}}{nK^{(1)}} \quad \text{and} \quad D^{(n)} = \frac{\bar{C}^{(n)}}{nK^{(1)}} \quad (10)$$

where, in general,  $K$  (without an overbar) designates the static stiffness while  $\bar{K}$  (with an overbar) stands for the dynamic stiffness. Note that at zero frequency  $k^{(n)}$  reduces to the familiar static group efficiency factor.

In Figure 4 the predictions of the developed simple analytical method compare very well with the rigorous solution of Kaynia.<sup>4</sup> Notice in particular the successful prediction of some of the detailed trends arising from pile-soil-pile interaction. The agreement for other pile group configurations (not shown herein)<sup>20</sup> is also invariably satisfactory, although not always as remarkable as that for the pile groups of Figure 4. Some noticeable discrepancies ( $\approx 25$  per cent) in the resonant peak values start appearing as the number,  $n$ , of interacting piles increases to 16 (i.e. for a  $4 \times 4$  pile group). But even in that case the prediction of the frequency-dependent distribution of the total applied load among the individual piles is, for all practical purposes, in good accord with Kaynia.<sup>4</sup> See Reference 20 for a detailed discussion of the phenomena observed in Figure 4, and for more results on homogeneous soils.

PILE-TO-PILE INTERACTION IN NON-HOMOGENEOUS SOIL: (a) RIGID PILES

It has been frequently suggested in the geotechnical literature that the strong interaction effects computed by the various theoretical methods for static or dynamic loads may not be realistic. The assumption of a homogeneous elastic soil is held responsible for exaggerating the influence of one pile on another. Indeed, in many real-life situations: (i) the soil stiffness increases with depth instead of remaining constant, while (ii) pile installation effects and non-linear soil behaviour near the pile shaft tend to produce radial changes in the effective soil stiffness. This section studies the effect only of vertical non-homogeneity [factor (i)] on the axial response of pile groups. (Reference is made to Veletsos and Dotson<sup>30</sup> and Sheta and Novak<sup>7</sup> for ways to introduce radial inhomogeneity in approximate modelling pile installation and non-linear effects on the impedance of single piles and pile groups, respectively.)

It is assumed that the soil moduli  $G_s$  and  $E_s$  increase with depth in a continuous form:

$$G_s(z) = G_0 \left( 1 + \frac{z}{z_0} \right)^m \tag{11}$$

with 
$$m \geq 0 \tag{12}$$

in which  $G_0$  = the surface shear modulus, at  $z = 0$  (Figure 1), and  $z_0$  is varied parametrically. Poisson's ratio and mass density are retained constant. While the method is subsequently developed for an arbitrary  $m$ , results are presented only for three characteristic values:  $m = 1/2$ , representative of cohesionless soil deposits;  $m = 1$ , representative of deposits of saturated normally-consolidated clays; and  $m = 2$ , representing deposits with density rapidly increasing with depth.

Refer now to Figure 5. As the (active) pile 'a' undergoes a vertical rigid-body oscillation,  $W_{11} \exp(i\omega t)$ , SV waves are emitted from every elementary surface of thickness  $\delta z$ , located at a depth  $z$  from the ground surface. The directions of propagation of these waves (the wave 'rays') are not straight lines as in a homogeneous medium. Snell's law of refraction

$$\frac{\sin[\theta(z')]}{V_s(z')} = \text{constant} \tag{13}$$

requires that each wave ray be a curve, forming a continuously changing angle  $\theta$  with the vertical axis, such that at each depth  $z'$  from the surface

$$\frac{d\theta}{ds} = \frac{dV_s(z') \sin \theta(z')}{dz' V_s(z')} \tag{14}$$

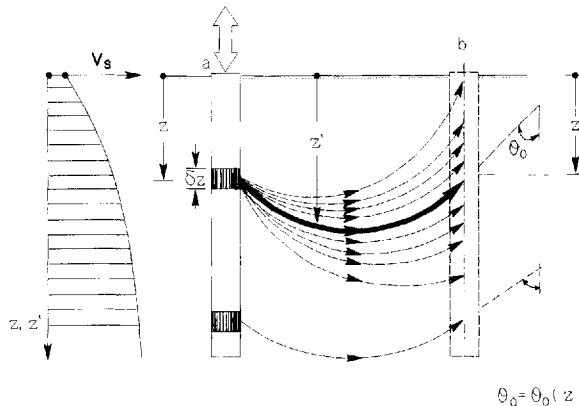


Figure 5. In a non-homogeneous soil with wave velocity increasing continuously with depth, waves emitted from a differential element on the shaft of an oscillating pile follow curved rays striking the neighbouring pile at various angles. The predominant assumption of the present method is that these wave rays can be replaced by a single 'average' ray with the shown geometric characteristics

in which  $ds$  is measured along the ray path, and  $V_s(z')$  is the S-wave velocity at the corresponding depth  $z'$ . Recognizing  $d\theta/ds$  as the curvature of the ray, it is evident that the shape of each ray depends on the value of  $m$ , which controls the modulus variation with depth [equation (11)]. For example, when  $m = 2$  the velocity is a linear function of depth, leading to a constant curvature and thereby to a circular ray path.

In general, several wave rays may originate at the particular depth to strike the (passive) pile 'b' at different elevations. In the interest of simplicity, it is assumed that these rays can be replaced by a single 'average' ray. To be somewhat consistent with the earlier assumption of horizontally propagating waves in a homogeneous medium, the 'average' ray is selected as the one striking pile 'b' at an elevation  $z$  equal to that at which the ray originated. Hence, the 'average' ray is symmetric with respect to the two piles, and the angles,  $\theta_a$  and  $\theta_b$ , of emergence on the axis of pile 'b' and of immergence from the axis of pile 'a' coincide:  $\theta_a = \theta_b = \theta_0$ . Note that the final results are hardly sensitive to the foregoing choice for the 'average' ray; changing  $\theta_0$  by 25 per cent leads to interaction curves differing by a negligible 5 per cent.

The angle  $\theta_0$  and the axis-to-axis length  $l$  of the ray path are readily determined by integrating the differential equation (14). To this end,  $V_s(z')$  is first substituted from equation (11). Also, from Snell's law

$$\frac{\sin\theta(z')}{\sin\theta_0} \approx \frac{V(z')}{V(z)} = \left(\frac{z_0 + z'}{z_0 + z}\right)^{m/2} \quad (15)$$

where the approximation sign is for ignoring the difference between S-wave velocity at depth  $z$ , where the waves actually originate, and S-wave velocity at the depth of the hypothetical origin of the 'average' ray on the piles axis. With these substitutions one obtains the following implicit equation in  $\theta_0 = \theta_0(z)$ :

$$2 \int_{\theta_0}^{\pi/2} \sin^{2/m}(\theta) d\theta = \frac{mS}{2(z_0 + z)} \sin^{2/m}(\theta_0) \quad (16)$$

For an arbitrary value of  $m$  the integral in equation (16) can only be determined numerically. But for the three characteristic values of  $m$  studied herein,  $m = 1/2, 1$  and  $2$ , the integral is computed analytically. For instance, for  $m = 1$  equation (16) reduces to

$$\frac{S}{z_0 + z} \sin^2(\theta_0) - \sin(2\theta_0) - 2\theta_0 = \pi \quad (17)$$

Transcendental equations like the above are solved numerically for  $\theta_0$ , for every depth  $z$  along the pile. For the case of linearly increasing velocity with depth,  $m = 2$ ,  $\theta_0$  is derived in closed form:

$$\theta_0 = \arctan\left(2 \frac{z_0 + z}{S}\right) \quad (18)$$

which reveals that  $\theta_0$  increases with  $z$ , and thereby that the circular 'average' rays become flatter as the depth increases (Figure 4).

The length of the 'average' ray originating at depth  $z$  is

$$l = l(z) = 2 \int_0^{S/2} \frac{dx}{\sin\theta} = \frac{4}{m} \frac{z + z_0}{\sin^{2/m}(\theta_0)} \int_0^{\pi/2} \sin^{2/m-1}(\theta) d\theta \quad (19)$$

which, for the particular case of  $m = 1$ , reduces to

$$l = 4(z + z_0) \frac{\cos(\theta_0)}{\sin^2(\theta_0)} \quad (20)$$

while an arbitrary  $m$  requires a (simple) numerical integration.

Finally, it is assumed that the 'average' rays involve exclusively S waves, and that along their path the wave amplitude decays in form similar to the asymptotic radial decay of cylindrical waves in a homogeneous medium [recall equation (8)]. Thus, the vertical component of the displacement amplitude imposed on pile

'b' at depth  $z$ , due to waves emanating from pile 'a', is

$$W_{12}(z) \approx w_{11} \left( \frac{r_0}{l(z)} \right)^{1/2} \exp \left( -\beta \omega \frac{l(z)}{\bar{V}_s(z)} \right) \exp \left( -i \omega \frac{l(z)}{\bar{V}_s(z)} \right) \quad (21)$$

in which  $\bar{V}_s = \bar{V}_s(z)$  denotes the average velocity of the soil along the particular ray path. The closed-form approximation

$$\bar{V}_s(z) \approx V_s(z) \frac{1 + \sin \theta}{2} \quad (22)$$

is sufficient for the required level of accuracy of this (simplified) method.

Thus, while the waves are emitted from various depths of pile 'a' in phase and with identical amplitudes, i.e.  $w_{11}(z) = W_{11}$ , equation (21) reveals that when these waves eventually strike pile 'b' they are out of phase and have different amplitudes. But since pile 'b' is rigid, it experiences a vertical displacement approximately equal with the average of these individual wave-ray displacements,

$$W_{12} \approx \frac{1}{L} \int_0^L w_{12}(z) dz \quad (23)$$

whence the 'dynamic interaction factor' is obtained by a simple (numerical) integration:

$$\alpha_v \approx \left( \frac{S}{r_0} \right)^{-1/2} \frac{1}{L} \int_0^{L_0} \left( \frac{S}{l} \right)^{1/2} \exp \left( -\beta \omega \frac{l(z)}{\bar{V}_s} \right) \exp \left( -i \omega \frac{l}{\bar{V}_s} \right) dz \quad (24)$$

Notice that equation (24) is a generalized version of equation (8), to which it reduces when the deposit tends to a homogeneous one, i.e. as  $l(z) \rightarrow S$  and  $\bar{V}_s(z) \rightarrow V_s$ .

Equation (24) is sufficient for computing the dynamic vertical response of any group of relatively short and/or stiff piles that behave as 'rigid' piles (i.e. whose bottom displacement is at least 80 per cent of the top displacements).

#### PILE-TO-PILE INTERACTION IN NON-HOMOGENEOUS SOIL: (b) 'FLEXIBLE' PILES

In this more general case, the displacements along the axis of a vertically oscillating single pile are *not* uniform:  $w_{11}(z) \neq w_{11}(0) = W_{11}$ . The shape  $\psi_{11}$  of such a vertical profile, defined as the distribution of vertical displacements *normalized to a unit average displacement*, is a function of both depth and vibration frequency:

$$\psi_{11} = \frac{w_{11}(z)}{\frac{1}{L} \int_0^L w_{11}(z) dz} = \psi_{11}(z; \omega) \quad (25)$$

To arrive at a *very simple* yet sufficiently accurate solution, the dependence of  $\psi_{11}$  on frequency is neglected and use is made of the static ( $\omega = 0$ ) displacement profile, as derived from Randolph and Wroth:<sup>21</sup>

$$\psi_{11}(z; \omega) \approx \psi_{11}(z; 0) \approx \frac{\delta \cosh \left[ \delta \left( 1 - \frac{z}{L} \right) \right]}{\sinh(\delta)} \quad (26)$$

in which

$$\delta = 2\sqrt{2} \frac{L}{d} \left( \frac{G_s(L)}{\zeta E_p} \right)^{1/2} \quad (27)$$

$$\zeta = \ln \left[ 5(1 - \nu) \frac{L}{d} \chi \right] \quad (28)$$

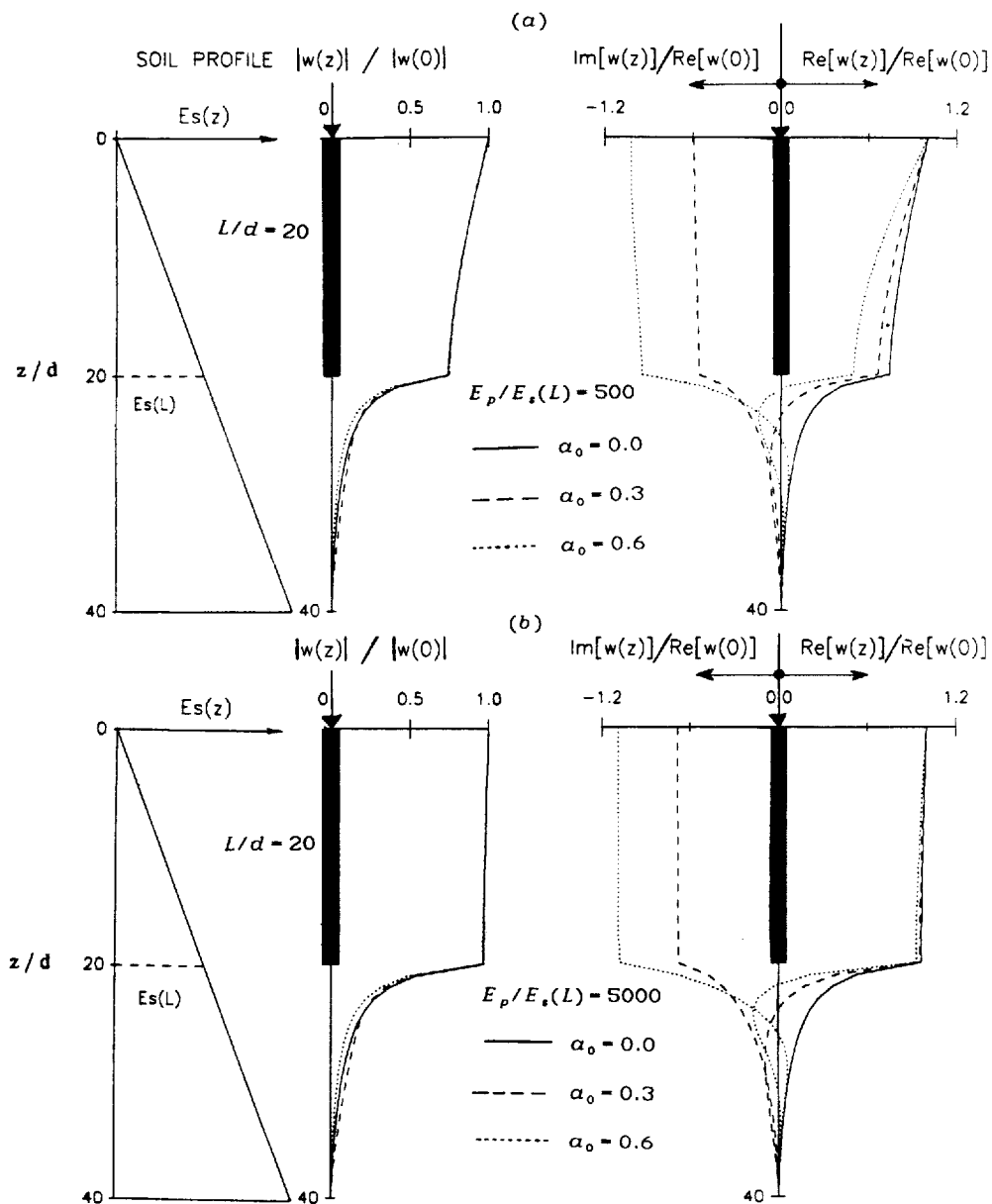


Figure 6. Distribution with depth of normalized dynamic and static vertical pile displacements (Absolute value, Imaginary part, Real part) for an  $L/d = 20$  pile in a deep non-homogeneous deposit with: (a)  $E_p/E_s(L) = 500$ ; and (b)  $E_p/E_s(L) = 5000$ . Displacements of soil under the pile are also plotted. Results obtained with a dynamic finite element formulation for the three values shown of the frequency factor. Notice the insensitivity of all displacement shapes to variation in frequency

where  $\chi = G_s(L/2)/G_s(L)$  reflects the degree of soil non-homogeneity (e.g.  $\chi = 1$  for homogeneous soil,  $\chi = 0.50$  with modulus proportional to depth, etc.) This is a reasonable *engineering* approximation for two reasons, elucidated with the help of Figure 6: (a) the shape of the absolute value of pile displacements is quite insensitive to variations in frequency (that is, frequency influences mainly the size of displacement amplitudes rather than the shape); (b) while the relative importance of the  $90^\circ$ -out-of-phase (imaginary) components of displacement increases with increasing frequency, the shape of their distribution with depth is also insensitive

to frequency. Thus, for at least  $E_p/E_s(L) \geq 500$ , the shapes of the real part, imaginary part and the absolute value of pile displacements are all fairly similar, hardly influenced by frequency changes. Therefore, the approximation of equation (26) is expected to lead to realistic results.

The waves emitted from all points of pile 'a' are in phase, in view of the still large cutoff frequency below which the phase velocity down the pile is nearly infinite. Propagating along the 'average' rays, such waves strike pile 'b' with vertical amplitudes:

$$w_{12}(z) \approx w_{11}(z) \left( \frac{r_0}{l} \right)^{1/2} \exp \left( -\beta \omega \frac{l}{V_s} \right) \exp \left( -i \omega \frac{l}{V} \right) \quad (29)$$

in which

$$w_{11}(z) \approx \psi_{11}(z; 0) \bar{W}_{11} \quad (30)$$

with  $\psi_{11}(z; 0)$  given by equations (24)–(26) and  $\bar{W}_{11}$  being the average displacement of pile 'a'; the other terms are as explained for equation (19).

Finally the 'dynamic interaction factor' is obtained from the following simple integration:

$$\alpha_v \approx \left( \frac{S}{r_0} \right)^{1/2} \frac{1}{L} \int_0^L \left( \frac{S}{l} \right)^{1/2} \psi_{11}(z; 0) \exp \left( -\beta \omega \frac{l}{V_s} \right) \exp \left( -i \omega \frac{l}{V_s} \right) dz \quad (31)$$

## PARAMETRIC RESULTS AND COMPARISONS

### *Comparison with results of more rigorous solutions*

It is imperative to substantiate the (engineering) accuracy of the developed simplified method through comparisons with rigorous solutions. Few such solutions seem to be presently available for pile groups in non-homogeneous soil deposits. One of them, by Banerjee and Sen,<sup>16</sup> is based on a hybrid boundary-element formulation and makes use of closed-form Green's functions for harmonic loads applied within a multi-layered deposit; these functions were derived by Kausel<sup>31</sup> and require a very fine discretization of the soil deposit into horizontal uniform sublayers.

The frequency variation of the complex dynamic interaction factor,  $\alpha_v = \text{Real}(\alpha_v) + i \text{Imaginary}(\alpha_v)$ , computed with equation (22), is compared in Figure 7 with that presented in Reference 16. The results refer to a deposit with soil modulus proportional to depth ( $m = 1$ ,  $G_s(0)/G_s(L) = 0$ ) and a practically rigid pile with  $E_p/E_s(L) = 10000$ . Two pile-separation distances are considered,  $S = 5d$  and  $S = 10d$ , while the frequency is non-dimensionalized with the S-wave velocity at the pile tip,  $V_s(L)$ , to give a frequency factor:

$$a_0 = \frac{\omega d}{V_s(L)} \quad (32)$$

The agreement between the two solutions is quite satisfactory. A noticeable discrepancy: the 'interference' peaks and valleys as predicted by the developed simple method occur at slightly greater frequencies than those of the Banerjee-Sen solution.

The implications of such a discrepancy are explored in Figure 8 where the stiffness and damping group factors,  $k^{(2)}$  and  $D^{(2)}$ , of a two-pile group are plotted versus  $a_0$ . The two sets of predictions now appear to be in much better accord, since their differences hardly exceed a mere 10 per cent. To provide a yardstick for the desired accuracy, Figure 8 also portrays the pile group factors for a *homogeneous* deposit, the shear modulus of which equals the average shear modulus,  $G_s(L/2)$ , of the non-homogeneous stratum. Note that such a halfspace is frequently used in practice to approximate non-homogeneous profiles and in fact, to arrive at reasonably good estimates of the *static* pile-to-pile interaction,<sup>32</sup> as is the case in this figure. However, it is clear that significant differences exist between the *dynamic* pile-group responses in the two media. These differences will be discussed later herein.

Another set of published boundary-element results<sup>32</sup> was found for the distribution of the total axial load among the individual piles of a square  $3 \times 3$  rigidly capped group. In addition, the Green's-function-based

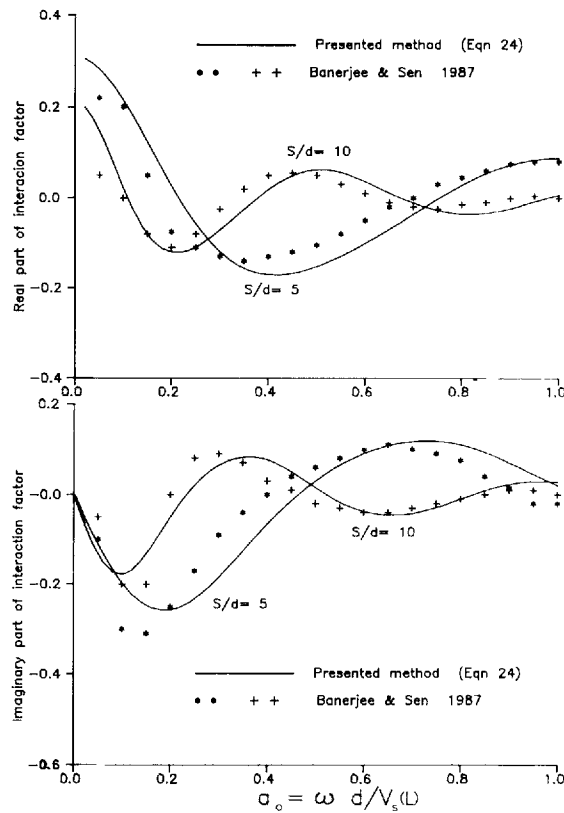


Figure 7. Non-homogeneous soil deposit with modulus proportional to depth: Real and Imaginary parts of the pile-to-pile interaction factor  $\alpha$ , (computed from equation (24) for two separation distances) are plotted as function of frequency and compared with results of a more rigorous formulation

method of Kaynia<sup>4</sup> was utilized for the same problem. Figure 9 compares the results of the three methods, for  $S/d = 4$ . Notice how sensitive the axial load distribution is to variations in frequency. For *static* and low frequency excitation the corner piles carry the largest portion of the applied load: their force amplitude  $F_1$  is about 1.4 times the average applied force. By contrast, at the same low frequencies the central pile carries a very small fraction of the load. (In fact, when the piles are too closely spaced ( $S = 2D$ ) our method predicts that the centre pile would essentially carry no load under static or low frequency excitation. The reason, as pointed out by Scott,<sup>19</sup> is that the soil around the central pile 'tends to drag this pile down, so that rather than resisting the applied load it is acting in the same direction',<sup>19</sup> hence, the pile can comply with the rigid-body settlement of the group even if it carries very little or no load.)

However, this picture changes at *higher frequencies* as waves emanating from other piles affect the response, producing undulations in the individual pile load sharing curves, as was unveiled by Sheta and Novak.<sup>7</sup> The central pile is particularly sensitive to such wave interferences, since the waves emitted by the surrounding eight piles hit this pile with not very different phases, in view of the similar spacings ( $S$  for four of them and  $S\sqrt{2}$  for the other four). Hence their (favourable or unfavourable) effects add up 'constructively'. As an example, assume, for a rough estimate, that the average length of the ray paths is 25 per cent greater than the respective pile spacing; then at wavelengths  $\lambda \approx \lambda_c$ , where

$$\lambda_c = 2 \frac{1.25S + 1.25\sqrt{2}S}{2} \approx 3S \quad (33)$$

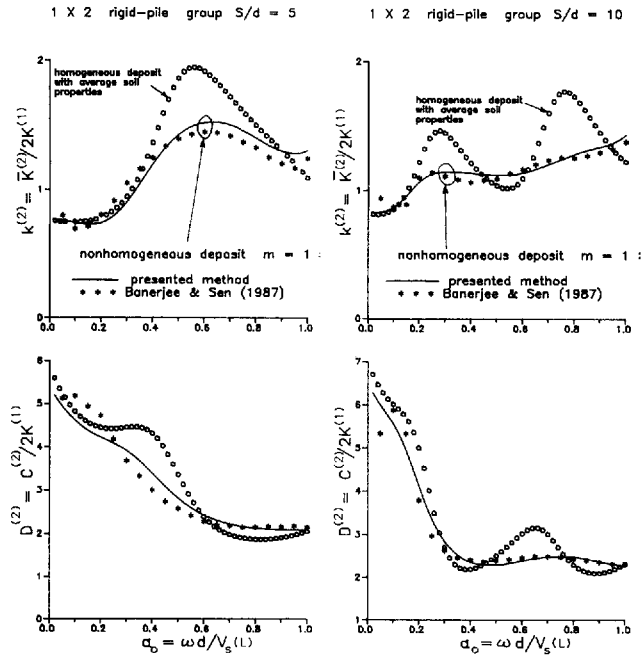


Figure 8. Comparison of stiffness and damping factors of a two-pile group with  $S = 5d$  (left) and  $S = 10d$  (right). The continuous line and the star points correspond to a non-homogeneous soil with modulus proportional to depth, and were obtained using the interaction factors of the presented method and of Banerjee and Sen which are shown in Figure 7. The circles are for a homogeneous deposit with shear modulus equal to  $G_s(L/2)$

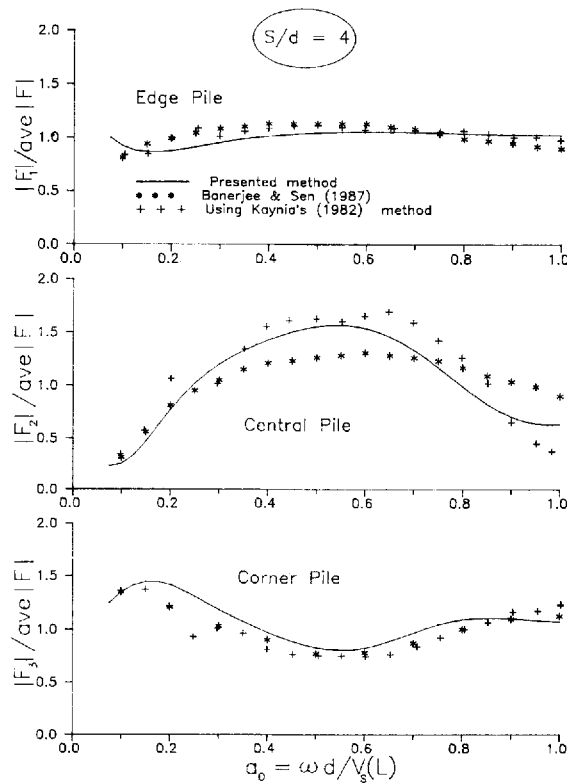


Figure 9. Variation with frequency of the distribution of axial force amplitudes carried by the corner, centre and edge pile in a  $3 \times 3$  rigidly-capped pile group: comparison of the developed simple method with the solution of Banerjee and Sen<sup>16</sup> and of Kaynia<sup>4</sup> and personal communication, State University of New York at Buffalo, Feb. 1989

which corresponds to frequency  $a_0 \approx a_{0,c}$ :

$$a_{0,c} = \frac{2\pi S}{(S/d)\lambda_c} \approx \frac{2.1}{(S/d)} \quad (34)$$

the central pile is pushed upward by most of the arriving waves with nearly their maximum amplitude, when its own load pushes downward. As a consequence, only by increasing its share of the total applied load can this pile be forced to follow the uniform displacement of the rigid cap. Equation (29) yields  $a_{0,c} \approx 0.52$  when  $S/d = 4$ . Indeed, around this frequency Figure 9 shows that  $F_2$  of the centre pile rises to a peak of 1.5 times the average load, while the share of the corner piles drops down to 75 per cent of the average load—a clear reversal of the static situation.

Evidently, the developed simple method gives results that are in substantial agreement (both qualitative and quantitative) with more rigorous formulations. Discrepancies between two more rigorous formulations may, in fact, exceed the inaccuracy of the simple method.

### EFFECT OF SOIL NON-HOMOGENEITY, GROUP CONFIGURATION AND PILE FLEXIBILITY

To further elucidate the role of soil non-homogeneity, Figures 10–13 plot as functions of  $a_0$  the stiffness and damping group factors for a number of square and linear pile group configurations and three separation distances. Figures 10 and 11 should be contrasted with Figures 4(a) and 4(b) corresponding to a homogeneous stratum. A similar comparison is displayed in Figure 8 for a two-pile group.

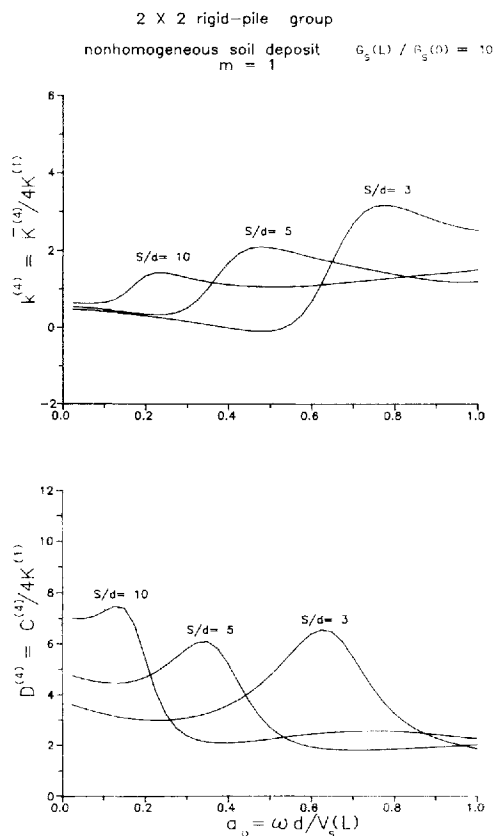


Figure 10. Effect of frequency and pile separation distance on the impedance of a group of 2 × 2 rigid and rigidly-capped piles in a non-homogeneous soil deposit (obtained with the present method)

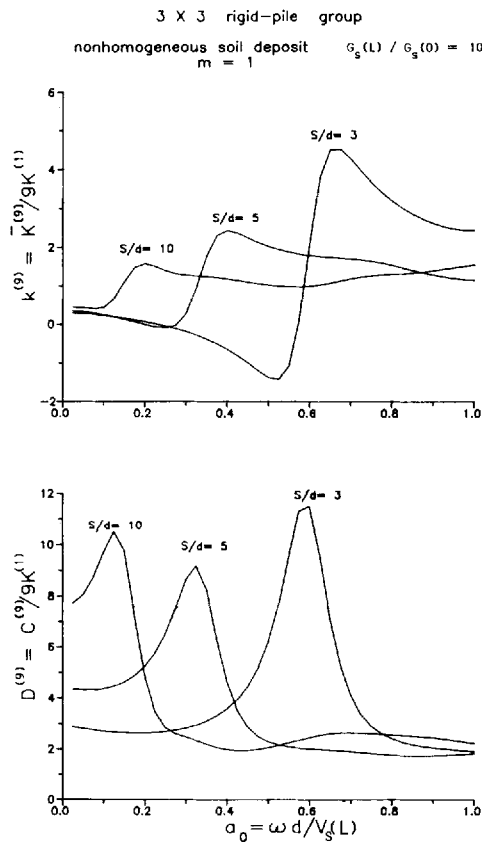


Figure 11. Effect of frequency and pile separation distance on the impedance of a group of 3 x 3 rigid and rigidly-capped piles in a non-homogeneous soil deposit (obtained with the present method)

Evidently, in non-homogeneous soils, the interference peaks of the pile-group stiffness tend to become shorter and flatter than those associated with homogeneous soil. There are believed to be two reasons:

1. The distances  $l = l(z)$  that the waves traverse along all the rays from pile 'a' to pile 'b' in a non-homogeneous medium exceed the distance  $S$  travelled in a homogeneous medium. Hence, the amplitudes of the incident waves, which decay as  $l^{-1/2}$  and  $S^{-1/2}$  in the two media, are relatively lower and tend to produce a smaller interaction effect in non-homogeneous soils. The differences that may arise from different damping decay terms  $\exp(-\beta\omega l/\bar{V}_s)$  and  $\exp(-\beta\omega S/\bar{V}_s)$  in the two media are not clear cut, because, while  $l$  always exceeds  $S$ ,  $\bar{V}_s = \bar{V}_s(z)$  may be larger or smaller than the homogeneous wave velocity  $V_s$ , depending on the location  $z$ .
2. In the homogeneous soil, the waves emitted from the various points along pile 'a' arrive on pile 'b' exactly in phase [a single  $\exp(-i\omega S/\bar{V}_s)$  term in equation (8)]. Thus, when this phase is  $180^\circ$  different from the phase of pile 'b' under its own load, it tends to produce the relatively sharp-and-high peaks seen in Figures 4 and 8. By contrast, in a strongly non-homogeneous medium the incident waves upon pile 'b' are not in phase; as reflected in the term  $\exp[-i\omega l(z)/\bar{V}_s(z)]$  of equation (19), phase differences stem primarily from the varying wave velocities  $\bar{V}_s(z)$ , and to a lesser extent from the varying length  $l(z)$  of the wave paths. Thus, it is not possible for all the incident waves to be  $180^\circ$  out of phase with the oscillation of pile 'b'; thereby, their superposition [equations (22) or (26)] leads to relatively short and flat peaks.

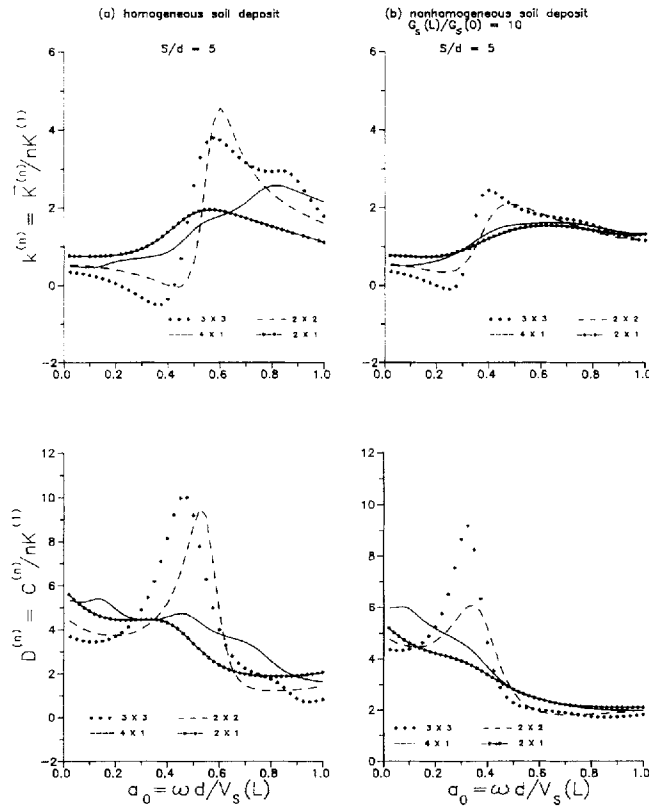


Figure 12. Effect of soil-modulus profile [(a) homogeneous, (b) non-homogeneous] and of pile group configuration ( $2 \times 1$ ,  $2 \times 2$ ,  $4 \times 1$ ,  $3 \times 3$ ) on the variation of stiffness and damping factors with frequency (obtained with the developed method)

The second of the foregoing two factors has been found to be the most significant, accounting for as much as 80 per cent of the computed differences in pile group response in the two media.

The importance of pile group configuration is studied on Figure 12(a) (homogeneous deposit) and Figure 12(b) (soil modulus increasing linearly with depth). Two square ( $2 \times 2$  and  $3 \times 3$ ) and two single-line ( $2 \times 1$  and  $4 \times 1$ ) configurations are examined. A fairly clear trend is emerging: in both profiles, the stiffness and damping of the square groups exhibit the strongest undulations, with the  $k$  factors reaching peak values of the order of 4 (in the homogeneous stratum) and 2 (in the non-homogeneous). By contrast, the corresponding peaks for the single-line groups reach only about 2 and 1.4, respectively. Another interesting observation is that the number of piles in a single-line group has only a small effect on the dynamic group factors. This behaviour, which holds true not only for the  $2 \times 1$  and  $4 \times 1$  groups studied in Figure 12 but essentially for any  $n \times 1$  group, has a rather simple explanation: every new pile 'a' that is added on an existing line of piles, 'b', 'c', . . . , emits waves that are  $180^\circ$  out of phase with the nearby pile 'b' when they are in phase with pile 'c'. Thus, the new 'constructive' and 'destructive' interferences occur simultaneously, i.e. at the same frequency, and their combined effect on  $k$  and  $D$  is hardly felt.

Finally, Figure 13 portrays the effect of pile flexibility on the dynamic interaction factor. The effect of decreasing pile flexural rigidity is insignificant, for  $L/d = 20$ ; and it remains rather small even for  $L/d = 40$ —in agreement with the findings for static loading researches.<sup>22</sup> Note, however, that the developed method may provide only a very crude estimate of the response of very long and flexible piles.

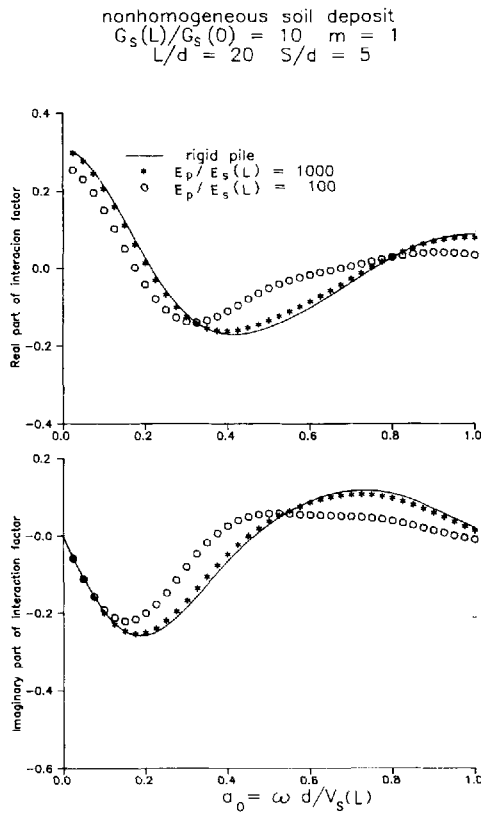


Figure 13. Effect of pile axial flexibility on the complex-valued interaction factor in non-homogeneous deposit (obtained with the developed method)

CONCLUSION

Physically-motivated approximations of the complicated wave fields around an oscillating pile have been introduced to solve the problem of pile-soil-pile interaction under axial harmonic loading. Both homogeneous and non-homogeneous soil deposits have been considered, and parametric results have been presented for the dynamic stiffness and damping of several pile groups. It is concluded that, owing to interaction effects, pile group impedances plotted against frequency will invariably exhibit peaks and valleys, the height and steepness of which decrease with increasing soil non-homogeneity. A companion paper deals with interaction under lateral and seismic loading.

ACKNOWLEDGEMENT

This work was supported by a research grant from the Secretariat for Research and Technology of the Greek government. The help we received from Dr Amir Kaynia in using his method to obtain the results of Figure 7, and by Mr Ke Fan in obtaining the results of Figures 3 and 6, is kindly acknowledged.

APPENDIX

List of main symbols

- $a_0 = \omega d / V_s$  dimensionless frequency for a homogeneous soil deposit
- $a_0 = \omega d / V_s(L)$  dimensionless frequency for a non-homogeneous soil deposit

$V_s$	shear wave velocity in a homogeneous soil deposit
$V_s(z)$	shear wave velocity in a non-homogeneous soil deposit at depth $z$
$G_s(z) = G_0(1 + z/z_0)^m$	soil shear modulus of non-homogeneous soil deposit
$G_s(L)$	soil shear modulus of non-homogeneous soil deposit at depth $L$
$G_s(0) = G_0$	soil shear modulus of non-homogeneous soil deposit at zero depth
$\mathcal{K} = \bar{K} + ia_0C$	dynamic impedance of a pile or a pile group
$\bar{K} = \bar{K}(a_0)$	dynamic stiffness of a pile group
$K = \bar{K}(0)$	static stiffness of a pile group
$k^{(n)} = K^{(n)}/nK^{(1)}$	dynamic stiffness group factor
$D^{(n)} = C^{(n)}/nK^{(1)}$	damping group factor
superscript $(n)$ :	indicates the total number of piles in a group

## REFERENCES

1. J. P. Wolf and G. A. Von Arx, 'Impedance function of group of vertical piles', *Proc. ASCE specialty conf. soil dyn. earthquake eng.* **2**, 1024-1041 (1978).
2. T. Nogami, 'Dynamic group effect of multiple piles under vertical vibration', *Proc. eng. mech. div ASCE speciality conf. Austin, Texas* 750-754 (1979).
3. T. Nogami, 'Dynamic stiffness and damping of pile groups in inhomogeneous soil', in *Dynamic Response of Pile Foundation* (Eds M. O'Neill and R. Dobry) ASCE, New York, 1980.
4. A. M. Kaynia, 'Dynamic stiffness and seismic response of pile groups', *Research Report R82-03*, Massachusetts Institute of Technology, 1982.
5. G. Waas and H. G. Hartmann, 'Analysis of pile foundations under dynamic loads', *Conf. struct. mech. reactor technol.* Paris (1981).
6. G. Waas and H. G. Hartmann, 'Seismic analysis of pile foundations including soil-pile-soil interaction', *Proc. 8th world conf. earthquake eng.* San Francisco, **5**, 55-62 (1984).
7. M. Sheta and M. Novak, 'Vertical vibration of pile groups', *J. geotech. eng. div. ASCE* **108**, 570-590 (1982).
8. T. R. Tyson and E. Kausel, 'Dynamic analysis of axisymmetric pile groups', *Research Report R83-07*, Massachusetts Institute of Technology, 1983.
9. T. Kagawa, 'Dynamic lateral pile group effects', *J. geotech. eng. div. ASCE* **109**, 1267-1285 (1983)
10. T. Nogami, 'Dynamic group effect in axial responses of grouped piles', *J. geotech. eng. div. ASCE* **109**, 225-243 (1983).
11. I. Sanchez-Salinerio, 'Dynamic stiffness of pile groups: Approximate solutions', *Geotechnical Engineering Report GR83-5*, University of Texas at Austin, 1983.
12. J. M. Roesset, 'Dynamic stiffness of pile groups', *Pile Foundations*, ASCE, New York, 1984.
13. C. H. Chen and J. Penzien, 'Seismic modeling of deep foundations', *Report No. EERC-84/19*, Earthquake Engineering Research Center, University of California, Berkeley, CA, 1984.
14. T. G. Davies, R. Sen and P. K. Banerjee, 'Dynamic behavior of pile group in inhomogeneous soil', *J. geotech. eng. div. ASCE* **111**, 1365-1379 (1985).
15. B. El Sharnouby and M. Novak, 'Static and low-frequency response of pile groups', *Can. geotech. j.* **22**, 79-94 (1985).
16. P. K. Banerjee and R. Sen, 'Dynamic behavior of axially and laterally loaded piles and pile groups', *Dynamic Behaviour of Foundations and Buried Structures*, Elsevier, New York, 1987, pp. 95-113.
17. H. G. Poulos and E. H. Davis, *Pile Foundation Analysis and Design*, Wiley, New York, 1980.
18. R. Butterfield and P. K. Banerjee, 'The elastic analysis of compressible piles and pile groups', *Geotechnique* **21**, 43-60 (1971).
19. R. F. Scott, *Foundation Analysis*, Prentice-Hall, Englewood Cliffs, N.J., 1981.
20. R. Dobry and G. Gazetas, 'Simple method for dynamic stiffness and damping of floating pile groups', *Geotechnique* **38**, 557-574 (1988).
21. M. F. Randolph and C. P. Wroth, 'Analysis of deformation of vertically loaded piles', *J. geotech. eng. div. ASCE* **104**, 1465-1488 (1978).
22. M. F. Randolph and C. P. Wroth, 'An analysis of the vertical deformation of pile groups', *Geotechnique* **29**, 423-439 (1979).
23. M. Novak, 'Dynamic stiffness and damping of piles', *Can. geotech. j.* **11**, 574-598 (1974).
24. D. Angelides and J. M. Roesset, 'Dynamic stiffness of piles', *Numerical Methods in Offshore Piling*, Institution of Civil Engineers, London, 1980, pp. 75-82.
25. G. Gazetas and R. Dobry, 'Horizontal response of piles in layered soils', *J. geotech. eng. ASCE* **110**, 20-40 (1984).
26. H. Kanakari, 'Dynamic response of axially and seismically loaded piles', *M.S. Thesis*, SUNY at Buffalo, 1990.
27. J. P. Wolf, *Dynamic Soil-Structure Interaction*, Prentice-Hall, Englewood Cliffs, N.J., 1985, pp. 166-172.
28. J. P. Wolf, *Soil-Structure Interaction in the Time-Domain*, Prentice-Hall, Englewood Cliffs, N.J., 1988.
29. N. Makris and G. Gazetas, 'Phase velocities and displacement phase differences in a harmonically oscillating pile', *Technical Report NCEER-90*, SUNY at Buffalo, 1990.
30. A. S. Veletsos and K. W. Dotson, 'Vertical and torsional vibration of foundations in inhomogeneous media', *Technical Report NCEER-87-0010*, Rice University, 1987.
31. E. Kausel, 'An explicit solution for the Green Functions for dynamic loads in layered media', *Research Report R 81-13*, Massachusetts Institute of Technology, 1981.
32. P. K. Banerjee and T. G. Davies, 'Analysis of pile groups embedded in Gibson soil', *Proc. 9th int. conf. soil mech. found. eng.* Tokyo I, 318-386 (1977).